Stem Cell Research (2009) 3, 142–156

available at www.sciencedirect.com

ScienceDirect

www.elsevier.com/locate/scr

REGULAR ARTICLE

Enhancement of human embryonic stem cell pluripotency through inhibition of the mitochondrial respiratory chain

S. Varum[a,b], O. Momčilović[a,c], C. Castro[a,d], A. Ben-Yehudah[a,d], J. Ramalho-Santos[b,*], C.S. Navara[e,*]

[a] *Pittsburgh Development Center, University of Pittsburgh School of Medicine, Pittsburgh, PA, USA*
[b] *Center for Neuroscience and Cell Biology, Department of Life Sciences, School of Science and Technology, University of Coimbra, Portugal*
[c] *Department of Human Genetics, Graduate School of Public Health, University of Pittsburgh, Pittsburgh, PA, USA*
[d] *Department of Obstetrics, Gynecology and Reproductive Sciences, University of Pittsburgh School of Medicine, Pittsburgh, PA, USA*
[e] *Biology Department, University of Texas at San Antonio, San Antonio, TX 78249, USA*

Received 28 October 2008; received in revised form 24 July 2009; accepted 26 July 2009

Abstract Human embryonic stem cell (hESC) pluripotency has been reported by several groups to be best maintained by culture under physiological oxygen conditions. Building on that finding, we inhibited complex III of the mitochondrial respiratory chain using antimycin A or myxothiazol to examine if specifically targeting the mitochondria would have a similar beneficial result for the maintenance of pluripotency. hESCs grown in the presence of 20 nM antimycin A maintained a compact morphology with high nuclear/cytoplasmic ratios. Furthermore, real-time PCR analysis demonstrated that the levels of Nanog mRNA were elevated 2-fold in antimycin A-treated cells. Strikingly, antimycin A was also able to replace bFGF in the media without compromising pluripotency, as long as autocrine bFGF signaling was maintained. Further analysis using low-density quantitative PCR arrays showed that antimycin A treatment reduced the expression of genes associated with differentiation, possibly acting through a ROS-mediated pathway. These results demonstrate that modulation of mitochondrial function results in increased pluripotency of the cell population, and sheds new light on the mechanisms and signaling pathways modulating hESC pluripotency.

Introduction

The mechanisms underlying the maintenance of hESC self-renewal and pluripotency are complex and poorly understood. Furthermore, the mechanisms by which hESC and mouse embryonic stem cells (mESC) maintain pluripotency differ. Both leukemia inhibitory factor (LIF) and bone morphogenetic protein 4 (BMP 4) play important roles in the maintenance of mESC self-renewal via activation of Stat3 (Matsuda et al., 1999; Niwa et al., 1998; Ying et al., 2003). Conversely, LIF is not sufficient to maintain pluripotency of hESC (Daheron et al., 2004) and addition of BMP 4 to the culture media results in rapid differentiation (Xu et al., 2002). Instead, the combined actions of basic fibroblast growth factor (bFGF, FGF2) and

* Corresponding authors.
E-mail addresses: jramalho@ci.uc.pt (J. Ramalho-Santos), christopher.navara@utsa.edu (C.S. Navara).

1873-5061/$ – see front matter © 2009 Elsevier B.V. All rights reserved.
doi:10.1016/j.scr.2009.07.002

TGFβ/Activin/Nodal signaling pathways are believed to be critical to hESC self-renewal. Nearly all formulations for the routine culture of hESCs include exogenous bFGF, demonstrated to increase the cloning efficiency of hESCs maintained under serum-free conditions (Amit et al., 2000). When added at high concentrations bFGF supports hESC self-renewal under feeder-free conditions in the presence (Rosler et al., 2004; Xu C et al., 2005) or absence of conditioned media (Xu C et al., 2005). Several studies have also shown that the combined activities of Noggin and bFGF maintain hESC self-renewal in the absence of conditioned medium due to the suppression of BMP activity (Wang et al., 2005; Xu RH et al., 2005). Furthermore, Activin or Nodal appear to cooperate with bFGF to maintain hESC pluripotency in chemically defined media (Vallier et al., 2005).

In addition to media constituent requirements Ezashi et al. (Ezashi et al., 2005) demonstrated that culture of hESCs under low oxygen (O_2) tension (5%) reduced the appearance of spontaneous differentiation. This may be the normal physiological state, as early-stage mammalian embryos also develop under low O_2 concentrations (1.5–5.3%) until they implant in the uterine endometrium, when O_2 levels increase with vascularization (Fischer and Bavister, 1993). When cultured under low O_2 tension, mammalian cells decrease ATP production via oxidative phosphorylation in the mitochondria and increase glycolytic functions in order to meet energy demands. Studies of mitochondrial number and morphology in hESCs have demonstrated that undifferentiated hESCs have relatively few mitochondria in the cytoplasm and these mitochondria have few christae, an indication of immature morphology (St John et al., 2005; Oh et al., 2005; Cho et al., 2006). As hESCs differentiate the number of mitochondria with a mature morphology increases, concomitant with the ATP levels produced by oxidative phosphorylation (Cho et al., 2006). Taken together, these results suggest that inhibition of mitochondrial function may prevent differentiation, and thus modulate the maintenance of pluripotency.

In this study we tested this hypothesis by specifically inhibiting complex III of the mitochondrial respiratory chain using antimycin A, an antibiotic isolated from *Streptomyces* sp. Antimycin A specifically blocks the flow of electrons from semiquinone to ubiquinone in the quinone cycle of complex III, thus disrupting the proton gradient across the inner membrane of mitochondria and preventing O_2 consumption at complex IV as well as ATP formation. Complex III is also known to be a source of reactive oxygen species (ROS) production in the cell; predominantly superoxide anion (O_2^-), which when produced in moderate amounts activates hypoxic signaling pathways in the cell. Consequently, complex III is considered the O_2 sensor of the cell (Chandel et al., 2000; Guzy et al., 2005). Antimycin A treatment simultaneously decreases ATP production via oxidative phosphorylation and increases ROS formation.

Results

Antimycin A (20 nM) was added 48 h after passaging to hESC cultures (WA07) growing on mouse embryonic fibroblast feeder cells (MEFs) in standard culture media, and this treatment was maintained for 5 days (Fig. 1). hESCs grown under these conditions maintained a typical compact morphology with high nuclear-cytoplasmic ratio and colonies with well-defined borders, comparable to those in control cells (data not shown). To quantify the levels of pluripotency, we used real-time PCR for the well-characterized pluripotency transcription factors Nanog and POU5F1 (also known as Oct-4). hESCs treated with antimycin A showed a 2-fold increase in Nanog mRNA levels compared with control cells (Fig. 1a, $P<0.01$, $n=6$). Oct-4 mRNA levels were not statistically different (Fig. 1a). Similar results were obtained with the complex III inhibitor, myxothiazol, used at a concentration of 20 nM (data not shown).

To determine if the effects observed after addition of antimycin A to the culture media were sustained or only transient, hESCs were maintained for several passages (1–2 months) in the presence of antimycin A. hESCs grown under these conditions maintained good morphology throughout (Fig. 1d) and maintained a 2-fold elevation of Nanog mRNA ($P<0.05$, $n=3$) relative to controls. Again, Oct-4 mRNA levels were not significantly different from controls (Fig. 1a). Western blot analysis of these extended treatment cells showed that Nanog protein levels were also increased in antimycin A-treated cells (Fig. 1b); Oct-4 protein levels were not significantly different between treatments (Fig. 1c). To ensure that prolonged antimycin A treatment did not negatively impact the pluripotent phenotype, we characterized these cells by ICC for the pluripotency markers Oct-4, Nanog, and SSEA-4. Nanog and Oct-4 were both found in the nucleus of antimycin A-treated cells, and the cell surface marker SSEA-4 labeled colonies (Fig. 1d) similar to control cells.

To determine if antimycin A-treated cells retained the potential to differentiate *in vivo*, we injected hESCs treated with antimycin A for 9 passages into NOD/SCID mice to test their ability to form teratomas. Similar to hESCs maintained under standard conditions (not shown), antimycin A-treated cells were able to form teratomas exhibiting tissues of all three germ layers (Fig. 1e), including gastrointestinal tissue (endoderm), cartilage (mesoderm), and neuro ganglia (ectoderm). Finally, cells grown for extended periods (19 passages) in the presence of antimycin A also maintained a stable 46 XX karyotype (data not shown).

To exclude the possibility that the effect of antimycin A on Nanog expression was due to an increase in cell survival of pluripotent stem cells relative to differentiated cells, the levels of annexin V/PI-positive cells were determined by flow cytometry (Figs. 2a–c). There was no statistically significant difference in the percentage of viable cells between control (83.25 ± 2.15, Figs. 2a and c) and antimycin A (81.2 ± 9.9, Figs. 2b and c)-treated cells. Based on these results antimycin A does not appear to affect cell survival.

In addition, proliferation of hESCs was determined by BrdU incorporation into genomic DNA during the S phase of the cell cycle (Figs. 2d and e). No statistically significant difference was observed in the percentage of cells that incorporate BrdU between control and antimycin A-treated cells. In combination with the above results, antimycin A does not seem to affect cell death or proliferation of hESCs.

As discussed above, bFGF is a well-described factor important in the maintenance of pluripotency in hESCs, even supporting pluripotency in the absence of feeder cells or conditioned media when present at high concentrations

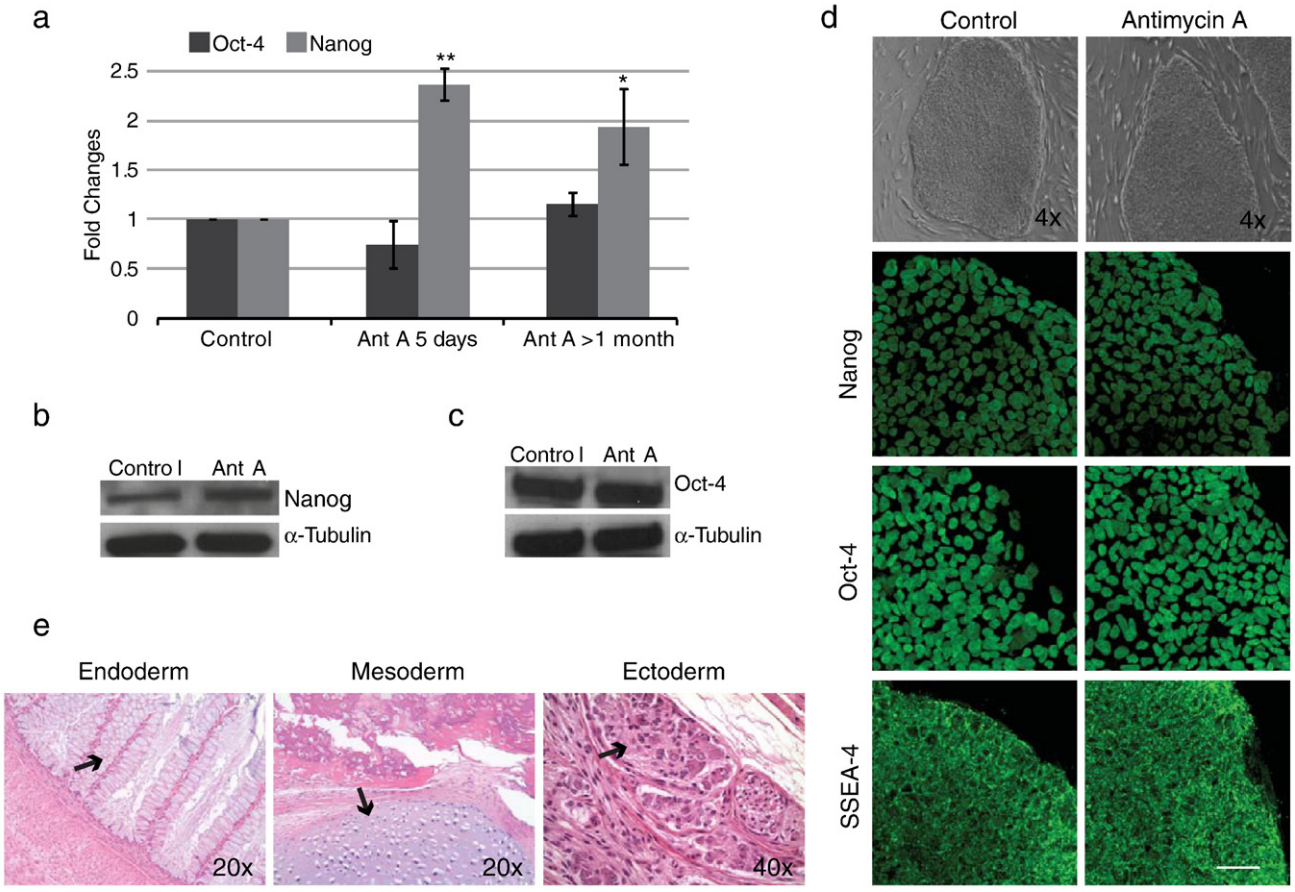

Figure 1 Analysis of pluripotency after antimycin A treatment. (a) Real-time PCR for the pluripotency markers Nanog and Oct-4 in hESC treated with antimycin A for 5 days or 4–8 passages. Statistically significant differences were determined by paired *t* test; $n=6$ and 3, respectively. $^{**}P<0.01$; $^{*}P<0.05$. (b,c) Western blot analysis for Nanog and Oct-4 protein levels in hESCs treated with antimycin A for 4–8 passages. (d) hESC morphology and pluripotency marker pattern expression after treatment with antimycin A for 4–8 passages, examined by phase contrast microscopy, ICC, and confocal laser scanning microscopy. (e) H and E staining of teratoma sections from hESCs treated with antimycin A for 9 passages. Abbreviations: Ant A, antimycin A; error bars, SEM. Scale bar, 50 μm.

(Wang et al., 2005; Xu et al., 2005). In order to better understand the beneficial effect of antimycin A we cultured hESCs on mouse feeders for 7 days using different combinations of antimycin A and bFGF and assayed Oct-4 expression by ICC. Colonies were divided into three categories according to the pattern of Oct-4 expression and quantified: totally positive colonies in which the majority of cells were positive for Oct-4 (Fig. 3a bottom left); partially positive colonies containing a significant quantity of both positive and negative cells (Fig. 3a bottom center); and negative colonies in which the majority of cells were negative for Oct-4 (Fig. 3a bottom right). At least 200 colonies were counted per treatment. As expected, removal of bFGF from the media resulted in a significant decrease in the number of totally positive colonies and an increase in the number of partially positive colonies (Fig. 3b; $P<0.001$), confirming the importance of this growth factor in the maintenance of healthy hESC colonies. Interestingly, when antimycin A was added to culture media lacking bFGF the numbers of totally positive colonies (65.9% vs 67.0%) and partially positive colonies (33.3% vs 32.6%) were indistinguishable from those under standard culture conditions (Fig. 3b), suggesting that addition of antimycin A maintains Oct-4 expression levels in culture conditions lacking bFGF. Surprisingly, the addition of both antimycin A and bFGF to the culture increased the number of totally positive colonies (86.8% vs 67.07%, $P<0.001$). The answer to this apparent contradiction is unknown but several factors may be involved. First, Western blotting and real-time PCR are unbiased quantitative analyses that probe an entire population of cells, while ICC as carried out here was inherently qualitative in terms of signal intensity, colony size, and colony heterogeneity (i.e., more or less positive cells in a colony), all of which could have played a role. Furthermore, subcellular localization of Oct-4 should also be considered. It is understood that during early differentiation of hESC Oct-4 localizes primarily in the cytoplasm instead of the nucleus, as is observed with undifferentiated hESCs. During human development Oct-4 is first observed cytoplasmically before localizing to the nucleus in the inner cell mass (Cauffman et al., 2005). In this case cells in which Oct-4 localizes to the cytoplasm will be counted as negative in our ICC analysis but would still be positive by Western blotting. Subcellular localization of Oct-4 may thus be a better assay of pluripotency than total

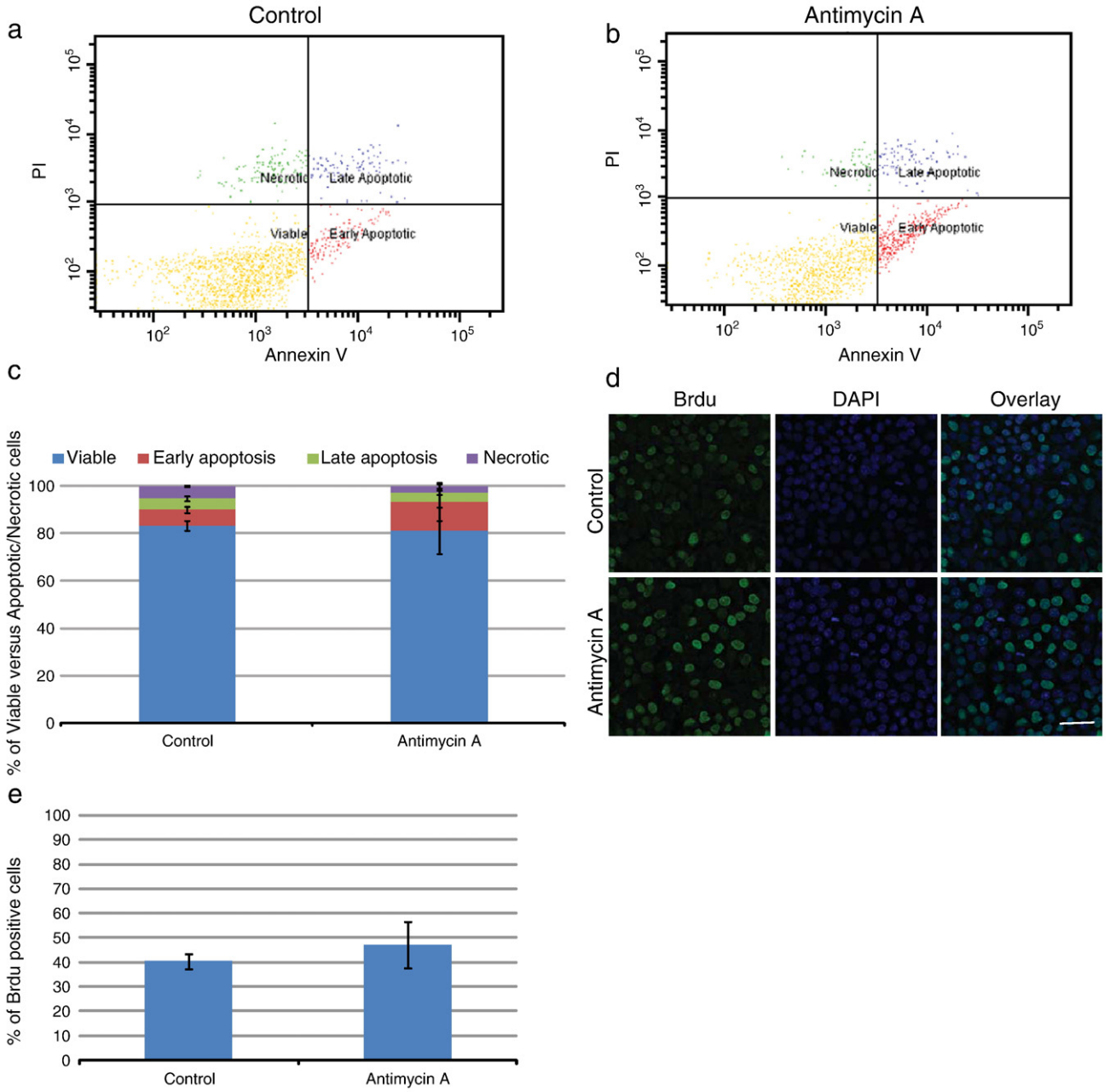

Figure 2 Analysis of apoptosis/necrosis and proliferation rates after antimycin A treatment. (a,b) Representative dot plots of flow cytometry for annexin V/PI of control and antimycin A-treated hESCs. Four populations were identified: viable cells (negative for both annexin V and PI); early apoptotic cells (positive for annexin V and negative for PI); late apoptoic cells (positive for both annexin V and PI); and necrotic cells (only positive for PI). (c) Percentage of the different cell populations in both control and antimycin A-treated cells, (d) BrdU incorporation in both control and antimycin A-treated hESCs, examined by confocal microscopy. (e) Percentage of BrdU-positive cells. Error bars, SEM. Scale bar, 50 μm.

cellular protein. Importantly, when performing double-labeling experiments for both Oct-4 and Nanog, the most striking effect of antimycin A treatment within single colonies was an increase of Oct-4+/Nanog+ cells (97% vs 70%) at the expense of the Oct-4+/Nanog− subpopulation (0.4% vs 23%). Finally, we performed real-time PCR for Nanog in both WA07 (Fig. 3c) and WA09 (Supplemental Fig. 1, carried out in a separate facility) for the conditions above. We observed that both cell lines are responsive to bFGF withdrawal demonstrated by a decrease in Nanog expression. In both cell lines antimycin A maintains Nanog expression on bFGF withdrawal, suggesting that this effect is not related to the particular characteristics of one hESC line.

One possible explanation for these results is that antimycin A induces bFGF secretion by feeders and/or hESCs. In order to address this point, bFGF concentration in the culture media was measured by ELISA (Supplemental Fig. 2). No bFGF secretion by mitomycin-inactivated MEFs was detected. The bFGF initially present in the media (4 ng/ml) was rapidly degraded/processed by the cells, as

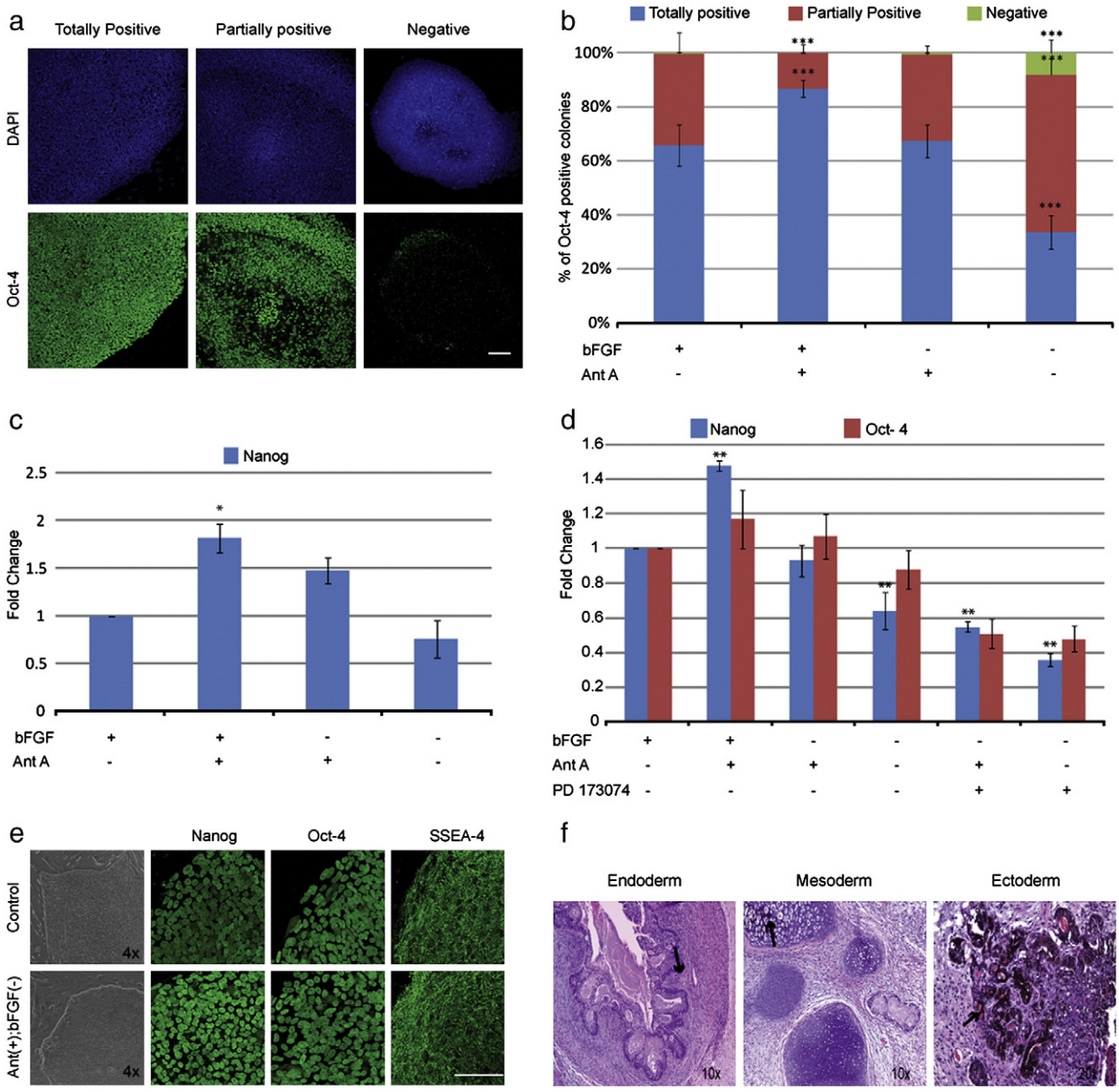

Figure 3 Analysis of pluripotency after antimycin A treatment in the absence of bFGF. (a) Oct-4 expression pattern categories in hESC analyzed by ICC and confocal laser scanning microscopy. (b) Percentage of totally positive, partially positive, and negative colonies for Oct-4 in antimycin A-treated cells in the presence or absence of bFGF for 7 days. Three independent experiments were performed, and at least 200 colonies total were analyzed per condition. Statistical significance was determined by chi-square test ***$P<0.001$. (c) Real-time PCR for Nanog in hESCs treated with different combinations of antimycin A and bFGF for 7 days. Statistical significance was determined by one-way ANOVA followed by Dunnet's multiple comparison test. *$P<0.05$. (d) Real-time PCR for Nanog and Oct-4 in hESCs maintained on Matrigel for 7 days with different combinations of bFGF, antimycin A, and PD173074. Statistical significance was determined by one-way ANOVA followed by Dunnet's multiple comparison test. **$P<0.01$. (e) hESC morphology and pluripotency marker pattern expression in cells treated with antimycin A in the absence of bFGF for 4–8 passages, analyzed as described in Fig. 1d. (f) H and E staining of teratomas from hESCs treated with antimycin A in the absence of bFGF for 33 passages. Abbreviations: Ant A, antimycin A; bFGF, basic fibroblast growth factor; (+), present; (–), absent. Error bars, SEM. Scale bar, 100 μm.

demonstrated in media concentrations of 65.92 ± 5.01 and 24.41 ± 3.58 pg/ml after 6 h or 24 h of culture, respectively (Supplemental Fig. 2a). These results are in accordance with the findings of Eiselleova et al. (Eiselleova et al., 2008) that showed, in contrast to human feeders, MEFs do not produce bFGF. Antimycin A treatment does not promote bFGF secretion by the MEFs as media concentrations are indistinguishable from controls (59.04 ± 3.94 and 27.31 ± 7.89 pg/ml) after 6 and 24 h of culture, respectively. In contrast to MEFs, hESCs appear to secrete bFGF into the media, since concentrations of 64.40 ± 36.72 pg/ml of bFGF were detected after 24 h of culture in media not supplemented with bFGF

(Supplemental Fig. 2b). These results are in accordance with the findings of Dvorak et al. (Dvorak and Hampl, 2005). bFGF production by hESCs was not affected by antimycin A treatment. These results indicate that the effect of antimycin A on pluripotency was not due to an increase in bFGF secretion by the feeders or by hESCs themselves.

These findings raise questions regarding the involvement of the bGF pathway in this effect. To address this issue we used the bFGF receptor inhibitor PD173074 (Mohammadi et al., 1998). hESCs were maintained on Matrigel for 7 days in different combinations of bFGF, PD173074, and antimycin A (Fig. 3d). Similar to what we observed for hESCs cultured on

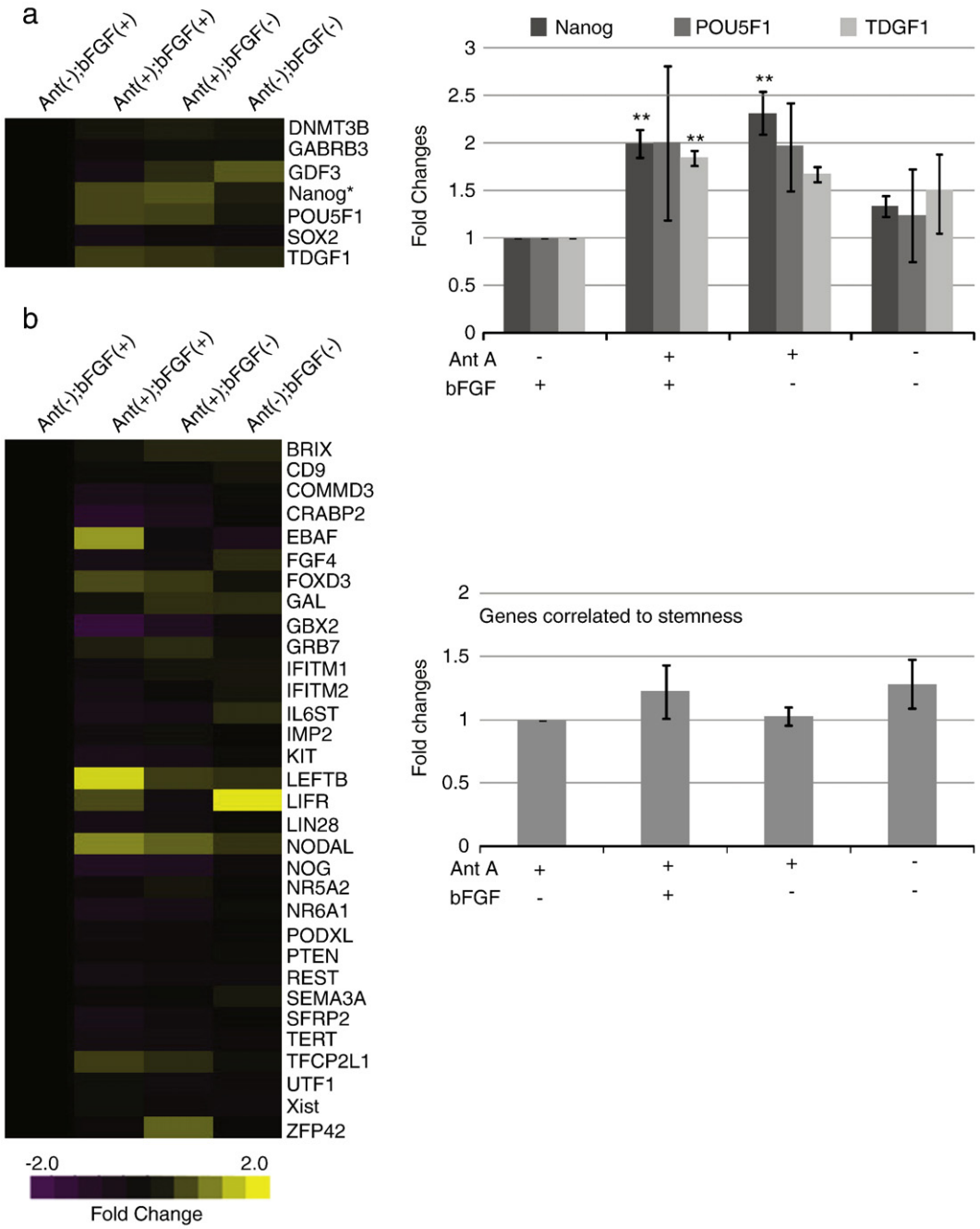

Figure 4 Pluripotency gene expression after antimycin A treatment in the presence or absence of bFGF Pluripotency gene expression profiles were analyzed by the TaqMan array human stem cell pluripotency panel. (a, left) Heat map for fold change differences of genes involved in the maintenance of pluripotency. (a, right) Bar graph of the fold changes differences observed for Oct-4, Nanog, and TDGF1. (b, left) Heat map for genes correlated with pluripotency. (b right) Bar graph of fold change averages of genes correlated with pluripotency. In this analysis an increase in expression is represented by the yellow color, whereas a decrease is represented by the purple color. Abbreviations: Ant A, antimycin A; bFGF, basic fibroblast growth factor; (+) presence; (−) absence. Statistically significant differences were determined by one-way ANOVA followed by Dunnet's multiple comparison test. Three independent experiments were performed. Error bars, SEM. $^{**}P<0.01$.

feeders, bFGF removal reduced Nanog expression (1.6-fold decrease) when compared to control cells (bFGF alone). Moreover, the addition of PD173074 promoted a significant decrease in Nanog and Oct-4 expression when compared to control cells (2.8- and 2.1-fold decrease, respectively). These results are in accordance with the findings of Dvorak et al. (Dvorak et al., 2005) who demonstrated a crucial role for the autocrine bFGF signaling pathway in the maintenance of hESC self-renewal. Treatment with antimycin A in the absence of bFGF maintained Nanog and Oct-4 mRNA expression at similar levels to controls; however, the expression of these markers decreased significantly on the addition of PD173074 (1.8- and 1.96-fold decrease for Nanog and Oct-4, respectively). Interestingly, the decrease in Nanog mRNA levels after the addition of PD173074 was less accentuated in the presence of antimycin A, perhaps suggesting that antimycin A functions through a different pathway than bFGF. These results indicate that, although antimycin A can maintain the expression levels of pluripotency markers in the absence of exogenous bFGF, it cannot maintain pluripotency when the endogenous bFGF pathway is inhibited, reinforcing the importance of the autocrine bFGF signaling pathway. Additionally, since antimycin A mitigated the effects of both exogenous bFGF removal and the inhibition of the endogenous bFGF pathway by PD173074, it is likely that antimycin A acts in a pathway separate from bFGF.

To determine if cells treated with antimycin A remain pluripotent in the absence of bFGF for prolonged periods of time, hESCs were treated with antimycin A in knockout media without bFGF for periods greater than 1 month. The best colonies under all conditions were manually passaged every 7 days. hESCs maintained under these conditions had a similar morphology to control cells, including tightly packed cells in colonies with well-defined borders (Fig. 3e). Immunocytochemical analysis demonstrated that these cells express the pluripotency markers Nanog, Oct-4, and SSEA-4 in similar patterns to control cells (Fig. 3e). We also evaluated the capacity of these cells to differentiate *in vivo*. Antimycin A-treated cells grown in the absence of exogenous bFGF (33 passages) generated teratomas exhibiting tissues from all three germ layers (Fig. 3f). These cells maintained a stable 46XX karyotype after prolonged culture (19 passages, data not shown).

To further investigate the role of antimycin A treatment on gene expression we used the TaqMan low-density array human stem cell pluripotency panel. These arrays contain 90 genes involved in maintenance of pluripotency or promotion of differentiation, along with 6 endogenous control genes (Adewumi et al., 2007). We maintained hESCs in different combinations of antimycin A and bFGF for more than 20 passages, and analyzed mRNA levels by real-time PCR. Among the genes analyzed were Nanog (Chambers et al., 2003; Mitsui et al., 2003), POUF51 (Nichols et al., 1998), and TDGF1 (Baldassarre et al., 1996), all critical for the maintenance of pluripotency. Consistent with our findings using single gene assays, treatment with antimycin A in the presence of bFGF resulted in a statistically significant 2-fold increase in Nanog expression, when analyzed with the low-density array (Fig. 4a; $n=3$; $P<0.01$). This difference was maintained in the absence of bFGF ($P<0.01$). TDGF1 was also significantly elevated after treatment with antimycin A (1.8-fold increase; $P<0.01$), while POU5F1 was elevated but not significantly. Both TDGF1 and POU5F1 were elevated in the absence of bFGF but did not rise to the level of significance. The other four pluripotency genes (SOX2, DMNT3B, GABRB3, and GDF3) on the array were not elevated and, surprisingly, removal of both antimycin A and bFGF did not significantly reduce expression levels of any of these genes (Fig. 4a, heatmap). When 32 genes correlated with pluripotency were examined, several genes were found to be amplified (Fig. 4b, heatmap), including EBAF, LEFTB, and NODAL, but several others decreased with antimycin A treatment including GBX2 and CRABP2. To compare these genes as a group across treatments, we averaged the fold changes across all 32 genes. No significant differences in the expression of these pluripotency correlated genes were observed between any treatments (Fig. 4b).

We also studied the expression of genes involved in differentiation. These genes were grouped according to their participation in endoderm (Fig. 5a), mesoderm (Fig. 5b), trophoblast (Fig. 5c), or ectoderm (Fig. 5d) differentiation and averaged as above. Antimycin A treatment in the absence of bFGF resulted in no statistical differences in the expression of differentiation genes in comparison to control cells (Figs. 5a–d). The addition of antimycin A in the presence of bFGF reduced the expression of differentiation genes in all categories (Figs. 5a–c), although only the decrease in ectoderm related genes was statistically significant (Fig. 5d, $P<0.01$, $n=3$). These results are in accordance with the findings of Vallier et al. (Vallier et al., 2009) who reported that Nanog overexpression prevents neuroectoderm differentiation. In contrast to the pluripotency genes whose expression did not change after withdrawal of bFGF and antimycin A, endoderm, trophoblast, and mesoderm genes were all significantly higher in the absence of these compounds (Figs. 5a–c; $P<0.01$, $n=3$). Only the ectodermal genes were unchanged in the absence of bFGF and antimycin A (Fig. 5d). This last result is in accordance with Stern (Stern, 2005) who reported that bFGF plays a crucial role in neuroectoderm specification in amphibian and chick embryos.

Antimycin A traditionally stimulates a shift in the metabolism from oxidative phosphorylation to glycolysis

Figure 5 Differentiation gene expression after antimycin A treatment in the presence or absence of bFGFs. Differentiation gene expression profiles were analyzed by the TaqMan array human stem cell pluripotency panel. (a–d left) Heat maps of fold change differences of differentiation genes involved in endoderm, mesoderm, trophoblast, and ectoderm specification. (a–d right) Bar graphs of fold changes average of differentiation genes involved in endoderm, mesoderm, trophoblast, and ectoderm specification. In this analysis an increase in expression is represented by the yellow color, whereas a decrease is represented by the purple color. Abbreviations: Ant, antimycin A; bFGF, basic fibroblast growth factor; (+) presence; (−) absence. Statistically significant differences were determined by one-way ANOVA followed by Dunnet's multiple comparison test. Three independent experiments were performed. Error bars, SEM. $^{**}P<0.01$.

(due to lower mitochondrial function) and promotes an increased superoxide generation at complex III (due to a lack of normal electron flow to oxygen, and thus the "leaking" of high-energy electrons from the transport chain). In order to determine if antimycin A treatment has the same effect in hESCs, the levels of adenine nucleotides (ATP, ADP, and AMP) were measured by high-performance liquid chromatography (HPLC) in control and antimycin A-treated hESCs. No

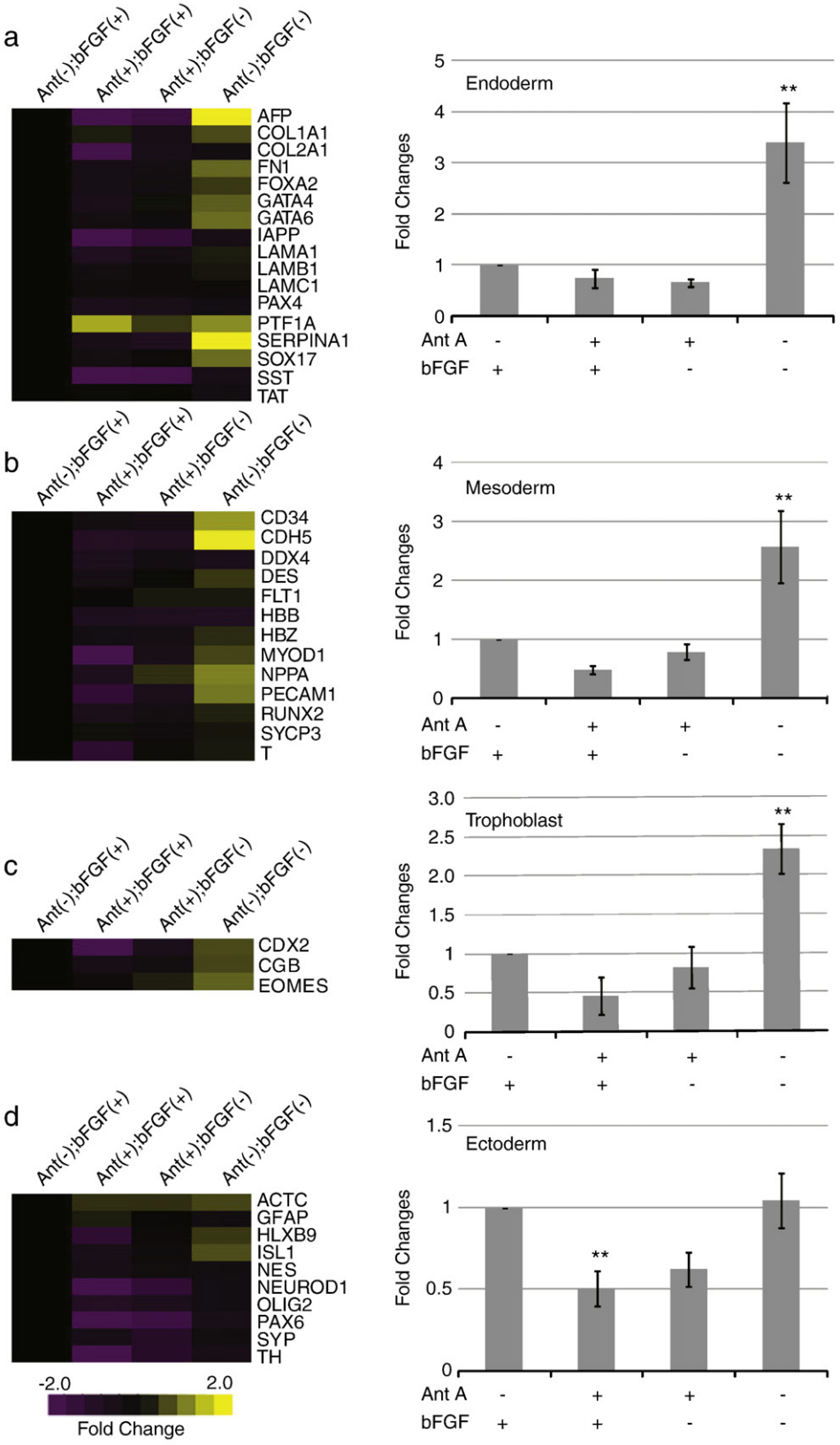

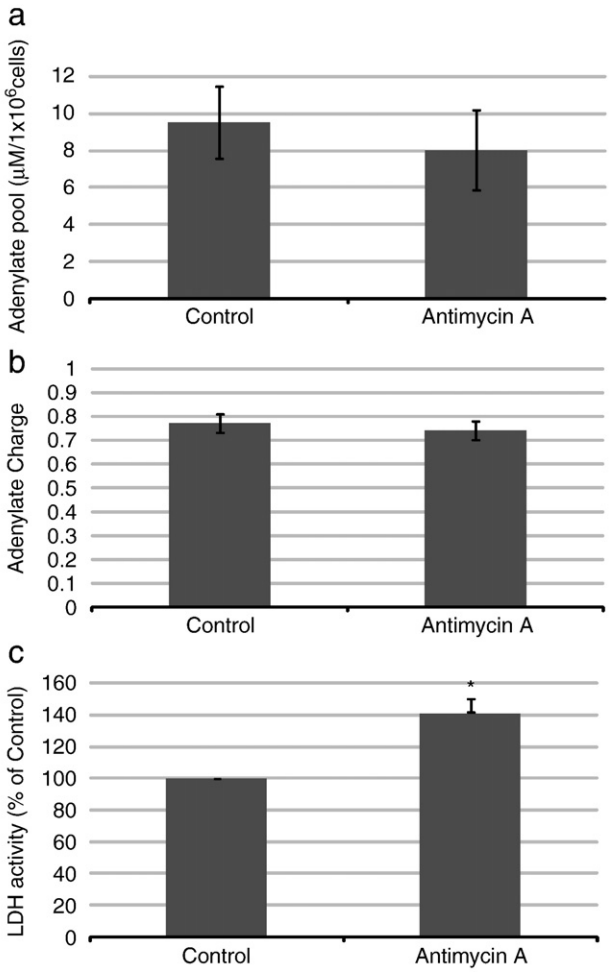

Figure 6 Energy metabolism analysis in antimycin A-treated hESCs. (a) Adenylate pool in antimycin A-treated cells. In order to determine the adenylate pool in the cell we performed reverse-phase high-performance liquid chromatography (HPLC) for ATP, ADP, and AMP. (b) Adenylate charge of antimycin A-treated cells. Adenylate energy charge was determined according to the following formula: ATP + 0.5ADP/(ATP+ADP+AMP). (c) Percentage of LDH activity in antimycin A-treated cells. Percentages were normalized to those found in control cells. Statistically significant differences were determined by paired *t* test. Three independent experiments were performed. Error bars, SEM. **P*<0.05.

significant differences in the adenylate pool or adenylate charge were observed between the two conditions (Figs. 6a and b). Lactate dehydrogenase (LDH) is an enzyme that converts pyruvate, the final product of glycolysis, to lactate when a decline in O_2 availability or impaired ATP production by mitochondria forces the cell into anaerobic metabolism, or when aerobic glycolysis is favored, as is the case in some cancers. Antimycin A-treated cells showed an increase of approximately 40% in the rates of LDH activity (Fig. 6c). These results indicate that antimycin A induces a shift in the metabolism toward glycolysis similar to what is observed in other cell types. However, hESCs cultured in the presence of antimycin A maintained ATP levels consistent with untreated cells.

As noted above, antimycin A increases the production of ROS in cells. To determine the effect of antimycin A on mitochondrial superoxide anion production in hESCs, we used MitoSox Red (Fig. 7). Cells treated with 20 nM antimycin A showed an increase of approximately 61 ± 20.7% in the number of positive cells for MitoSox Red when compared with control cells, as monitored by flow cytometry. This effect was dose dependent as treatment of hESCs with 2 μM of antimycin A increased the number of positive cells approximately 250 ± 16.3%. This effect was counteracted by the addition of MnTbap, a cell-permeable superoxide dismutase (SOD) mimetic which acts as a scavenger specifically targeting superoxide. Treatment with 50 μM MnTbap eliminated the effect of treatment with 20 nM antimycin A. MnTbap was also able to reduce the number of positive hESCs under control conditions (Figs. 7a and b).

Reactive oxygen species are important signaling molecules within the cell. To address whether the effect of antimycin A on pluripotency is mediated by ROS cells were maintained in different combinations of antimycin A and MnTbap and real-time PCR for Nanog was performed (Fig. 7c). MnTbap was able to partially abrogate the antimycin A-stimulated increase in Nanog expression, although no significant differences were observed between control and MnTbap-treated cells. These results suggest that superoxide anion generated at complex III is at least partially responsible for the effect of antimycin A on Nanog expression.

Discussion

Studies have demonstrated that hESCs cultured under low oxygen tension (1.5–5%) are better maintained in the undifferentiated state (Ezashi et al., 2005; Westfall et al., 2008). This suggests that a decrease in mitochondrial oxidative phosphorylation and an increase in ROS signaling under these conditions might be involved. We show here that this effect can be mimicked by directly inhibiting mitochondrial function in a way that is at least partially dependent on ROS formation. hESCs treated with 20 nM antimycin A maintained pluripotency not only as evidenced by immunocytochemical staining of the pluripotency markers but also as assayed by teratoma formation. Real-time PCR and Western blot analysis demonstrated that antimycin A-treated hESCs had elevated levels of both Nanog mRNA and protein. While a similar increase was observed for TDGF1 mRNA expression, no significant differences were observed for Oct-4 protein or mRNA. These results can best be explained by considering that, unlike the case for Oct-4, overexpression of Nanog is

Figure 7 Superoxide anion generation in antimycin A-treated hESCs. (a) Representative flow cytometry histograms demonstrating percentages of MitoSox Red-positive cells on treatments with different combinations of antimycin A and MnTbap. (b) Percentages of MitoSox Red-positive cells in control versus treated hESCs. Percentages were normalized to those found in control cells (c) Real-time PCR for Nanog of hESCs treated with different combinations of antimycin A and MnTbap. Statistical significance was determined by one-way ANOVA followed by Dunnet's multiple comparison test. Error bars, SEM. **P*<0.05; ****P*<0.01.

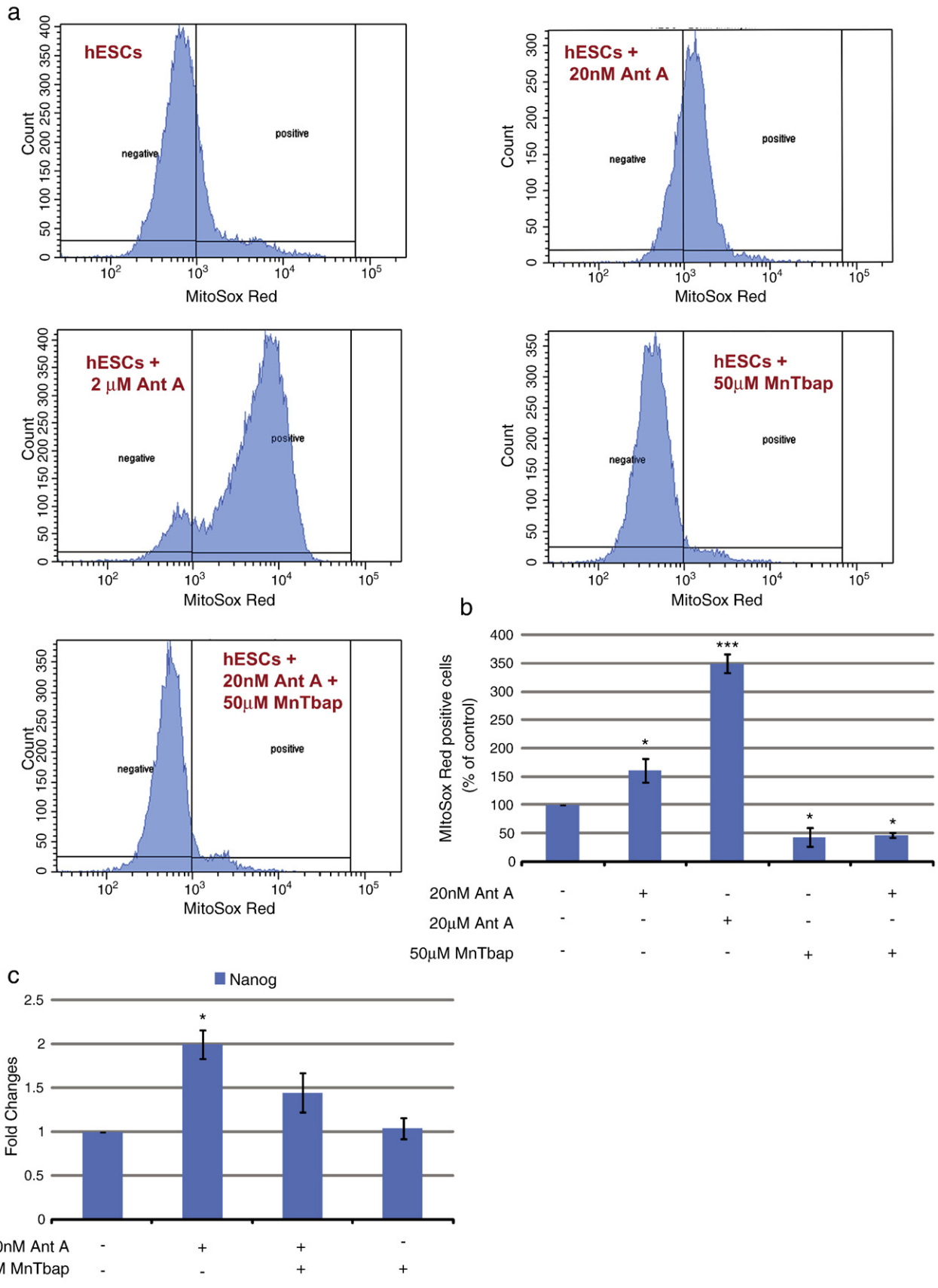
a
hESCs
negative
positive
Count
MitoSox Red
hESCs +
20nM Ant A
hESCs +
2 μM Ant A
hESCs +
50μM MnTbap
hESCs +
20nM Ant A +
50μM MnTbap
b
MitoSox Red positive cells
(% of control)
20nM Ant A
20μM Ant A
50μM MnTbap
c
Nanog
Fold Changes
20nM Ant A
50μM MnTbap

beneficial for the maintenance of pluripotency, namely preventing neuroectoderm differentiation induced by FGF signaling (Vallier et al., 2009). Others have shown that overexpression of Nanog allows culture in the absence of feeders (Darr et al., 2006) and circumvents the need for both TGFb and FGF signaling in the maintenance of pluripotency (Xu et al., 2008). In contrast Oct- 4 levels must be kept within defined ranges in order to maintain self-renewal of both mouse and human ESCs, as overexpression results in upregulation of markers involved in endoderm and mesoderm specification of both cell types (Rodriguez et al., 2007; Niwa et al., 2000) while, conversely, RNA interference targeting Oct-4 can trigger trophectoderm differentiation (Hay et al., 2004; Velkey et al., 2003; Matin et al., 2004). Additionally, Pan et al. (Pan et al., 2006) demonstrated that a steady-state concentration of Oct-4 maintains Nanog expression, whereas an elevated concentration of Oct-4 suppresses Nanog expression. Therefore, while upregulation of Nanog is globally beneficial to the maintenance of pluripotency, upregulation of Oct-4 can be detrimental and maintenance of the status quo is appropriate for Oct-4 expression. Taking into account these findings it seems that antimycin A does not increase Oct-4 expression above the steady-state present in pluripotent hESCs.

Very few growth factors have been identified as being necessary or sufficient for maintenance of hESC pluripotency, though one leading candidate is bFGF (Amit et al., 2000; Rosler et al., 2004; Xu et al., 2005). As bFGF and antimycin A both promote pluripotency, we were interested in determining if antimycin A could maintain pluripotency in the absence of bFGF. Treatment with antimycin A was able to alleviate the requirement for exogenous bFGF as there was no difference in the number of totally positive colonies between standard culture conditions and those including antimycin A but lacking bFGF. Furthermore, antimycin A was able to sustain Nanog expression on bFGF removal in both WA07 and WA09 cell lines, demonstrating that the effect is not ES line dependent. Antimycin A treatment failed to maintain pluripotency on the inhibition of the endogenous bFGF pathway, indicating the requirement for the endogenous bFGF pathway in the maintenance of pluripotency. The observation that antimycin A increases Nanog expression even when the endogenous pathway is suppressed suggests that antimycin A works through a pathway other than bFGF. Taken together, our results suggest that bFGF and antimycin A work through synergistic pathways to maintain pluripotency.

Cells cultured for several months in the presence of antimycin A and absence of exogenous bFGF remained pluripotent as assessed by ICC and teratoma formation. Furthermore, low-density array analysis showed that antimycin A treatment of hESCs cultured in the absence of bFGF resulted in an elevated expression of Nanog mRNA and maintained the expression of differentiation genes at similar levels to those found in control cells.

Our findings can be explained in light of morphological and functional changes that mitochondria undergo during early mammalian development. In the oocyte, mitochondria are spherical with few christae, whereas between the zygote and the morula stage, mitochondria become more elongated (Ramalho-Santos et al., 2009). At the blastocyst stage two distinct forms of mitochondria are present: mitochondria in the inner cell mass (ICM) are spherical and have low O_2 consumption, whereas those in the trophectoderm (TE) are elongated and have higher respiratory rates (Stern et al., 1971; Houghton, 2006). As hESCs are derived from the ICM, one should expect that they share these metabolic and morphological features. Indeed, it has been shown that undifferentiated hESCs have few mitochondria with an immature morphology, and a greater reliance on glycolysis (St John et al., 2005; Oh et al., 2005; Cho et al., 2006). As hESCs differentiate the number of mitochondria with a mature morphology increases, as well as ATP production by oxidative phosphorylation (Cho et al., 2006).

Finally, our results indicate that ROS produced at complex III of the mitochondrial electron transfer chain are at least partially responsible for the antimycin A effect on Nanog expression. Mitochondrial ROS constitute the major source of ROS in the cells and are produced as side products of oxidative phosphorylation. The involvement of ROS in deleterious processes such as DNA damage, changes in the native structure of proteins, and lipidic peroxidation of membranes has long been recognized. More recently, however, it has been recognized that ROS can modulate various intracellular signaling pathways through covalent modifications (so-called "redox signaling") of target molecules, thereby inducing changes in cells that are important in many physiological and pathophysiological processes (Finkel, 2003). In addition, there is a growing body of evidence that there is an increase in ROS production following the addition of various peptide growth factors to cells in culture, and that these ROS are a crucial component of downstream signaling. Our results demonstrate that antimycin A increases superoxide generation at complex III and that capture of superoxide anion by MnTbap partially abrogates the effect of antimycin A in Nanog expression, suggesting ROS as at least a partial modulator of antimycin A effect on pluripotency. Superoxide anion can rapidly convert to other reactive species and therefore not be captured by MnTbap, thus continuing to signal, which might also explain why MnTbap does not completely eliminate the antimycin A effect. This is in accordance with the reports of Carriere et al. (Carriere et al., 2004) demonstrating that antimycin A inhibited murine preadipocyte differentiation toward the adipocyte phenotype by increasing ROS formation at complex III. Indeed, several growth factor and cytokines such as bFGF and TGFβ are known to induce H_2O_2 generation in different cell types (Thannickal and Fanburg, 2000). Alternatively, the effect of antimycin A in Nanog expression could be a synergistic action between ROS production and a shift in oxidative metabolism toward glycolysis, which we have also demonstrated to take place. This latter hypothesis is in accordance with findings of Chung et al. (Chung et al., 2007) who showed that during the *in vitro* process of mESC differentiation, antimycin A inhibits oxidative phosphorylation and leads to a reduced appearance of beating cardiomyocytes. In addition, we cannot rule out the hypothesis that the effect of antimycin A on Nanog expression could be partially mediated by changes in calcium homeostasis. Indeed, Spitkovsky et al. (Spitkovsky et al., 2004) demonstrated that while antimycin A blocked cardiomyocyte differentiation by acting on calcium signaling, the use of KCN (an inhibitor of complex IV of the mitochondrial respiratory

chain) did not. Further work is required to pinpoint the exact mechanism(s) involved but our data provide the first evidence that modulation of mitochondrial function (probably acting through a ROS-dependent pathway) can influence the pluripotent state of hESCs.

Materials and methods

Human embryonic stem cell culture

WA07 cells (WiCell) were cultured under normoxic conditions (21% O_2 and 5% CO_2) in Knockout medium containing 80% Knockout Dulbecco's modified Eagle's medium (DMEM) (Invitrogen, Carslbad, CA) supplemented with 20% Knockout Serum Replacer (Invitrogen), 1 mM L-glutamine, 4 ng/ml basic human recombinant FGF, and 0.1 mM MEM nonessential amino acids, 50 μg/ml penicillin, and 50 μg/ml streptomycin (all from Invitrogen). Cells were passaged manually (Day 0) using a pulled glass needle and then plated onto mitomycin C-inactivated mouse embryonic fibroblast feeder cells (Specialty Media, Phillipsburgh, NJ). On Day 2, 20 nM antimycin A (Sigma-Aldrich, St. Louis, MO) was added and media were changed every other day and new drug was added. hESC culture on Matrigel (BD Biosciences) was performed as described previously (Xu et al., 2001). Briefly, human knockout medium was conditioned in MEFs and a total of 8 ng bFGF/ml was used to supplement the media. Matrigel was diluted according to manufacturer's instructions and was allowed to coat dishes for at least 30 min at room temperature before cells were added. In order to allow cells to plate, treatments were initiated at Day 2 after scraping and fresh media and drugs were added every other day. MnTbap and PD173074 (Mohammadi et al., 1998; Ying et al., 2008) were used at 50 μM and 100 nM, respectively.

Immunocytochemistry

Immunocytochemistry (ICC) for the standard pluripotency markers Oct-4, Nanog, and SSEA-4 was assessed as previously described (Navara et al., 2007). Only cells in which Oct-4 was localized in the nucleus were considered positive for this marker, whereas cytoplasmatic localization was considered as negative.

RNA extraction, RT PCR, and TaqMan low-density arrays

Total RNA extraction and PCR mixtures were prepared as previously described (Navara et al., 2007). Real-time PCR was performed using an ABI Prism 7700 (Applied Biosystems Incorporated, Foster City, CA). Taqman gene expression assays (Applied Biosystems) were used for Nanog, Oct-4, and β actin. Water and no RT samples were used as negative controls; all samples were run in triplicate. The TaqMan array human stem cell pluripotency panel (Applied Biosystems) was used following manufacturer's instructions. Nine (FGF5, KRT1, GCM1, HBB, WT1, GCG, INS, IPF1, MYF5) genes were excluded from our analysis due to very poor amplification in any sample. mRNA fold changes were calculated using the $-\Delta\Delta C_t$ method and normalized using β actin expression as endogenous control.

Western blotting

hESCs were collected manually in PBS and pelleted. Total protein extract was collected using RIPA buffer (Sigma) supplemented with 1 mM PMSF. Protein quantification was carried out using the Bradford assay (Bio-Rad Laboratories Inc., CA) and 10 μg of protein was separated by 12% SDS-PAGE. Primary antibodies used Nanog (Kamiya Biomedical Company) and Oct-4 (Santa Cruz Biotechnology). ECL Advance Western blot detection kit (Amersham Biosciences, Piscataway, NJ) was used for detection.

Teratoma formation

hESCs treated for prolonged periods of time with 20 nM of antimycin A either in the presence or in the absence of bFGF were injected into the testis of nonobese diabetic/severe combined immune deficient (NOD/SCID) mice. Three mice were injected per experiment as previously described (Navara et al., 2007).

Apoptosis/necrosis assay

hESCs were maintained on Matrigel and treated with antimycin A as previously described and apoptosis/necrosis rates were detected using the annexin V/PI apoptosis detection kit (BD Biosciences) following the manufacturer's instructions. Briefly, cells were washed with PBS and dissociated with Accutase followed by two washes in cold (4 °C) PBS. The amount of 1×10^6 cells was resuspended in 100 μl of binding buffer and 5 μl of both annexin V and PI was added. The mixture was incubated for 15 min at 25 °C in the dark followed by the addition of 400 μl binding buffer. Labeled cells were analyzed by flow cytometry (BD LSR II, BD Biosciences).

Measurement of hESC proliferation

hESC proliferation was determined by BrdU (Roche) incorporation into the genomic DNA during the S phase of the cell cycle. hESCs maintained on Matrigel were treated with antimycin A as previously described. At Day 6 after plating hESCs were incubated in medium containing BrdU for 3 h and washed three times with PBS. Cells were fixed and incorporated BrdU was detected with Anti-BrdU according to the manufacturer's instructions. Cells were imaged by confocal microscopy and at least 2500 cells were counted to determine number of cycling cells.

ATP measurement by HPLC

hESCs were maintained on Matrigel and antimycin A treated as previously described. Intracellular adenine nucleotides (ATP, ADP, and AMP) were determined as previously described (Amaral et al., 2006). In brief, adenine nucleotides were extracted with 0.6 M perchloric acid supplemented with 25 mM EDTA-Na. Cell supernatants were neutralized with 3 M KOH in 1.5 M Tris followed by centrifugation. Supernatants were assayed by HPLC. The detection wavelength was 254 nm, and the column was a Licophesfere100 RP108 5 μM (Merk). Adenylate

energy charge was calculated according to the following formula: ATP+0.5×ADP/(ATP+ADP+AMP).

Lactate dehydrogenase activity

Lactate dehydrogenase activity was determined using the QuantiChrom lactate dehydrogenase kit (Bio Assay Systems, CA) following the manufacturer's instructions. Cells were mechanically dissociated and lysed in 100 mM potassium phosphate containing 2 mM EDTA buffer and centrifuged and the resulting supernatants were assayed using the working reagent. Optical density was read at 565 nm immediately after the mixture of the sample and the working reagent, and also 25 min after addition. LDH activity was determined based on the following formula: LDH activity = $43.68 \times (OD_{S25} - OD_{S0}) / (OD_{calibrator} - OD_{H2O}) \times$ dilution factor.

Superoxide anion detection by MitoSox Red

hESCs were maintained on Matrigel for 7 days and treatments (antimycin A and/or MnTbap) were initiated at Day 2 after scraping. Fresh media and drugs were added every other day. On Day 7, cells were washed with PBS and dissociated with Accutase followed by two washes in PBS. Superoxide was detected using MitoSox Red (Invitrogen). Cells were suspended in media and incubated with 2.5 μM MitoSox Red for 30 min at 37 °C followed by one wash in PBS and subsequent analysis by flow cytometry.

Statistical analysis

Means and standard error of the mean were calculated and statistically significant differences were determined by paired *t* test, chi-square test, or one-way ANOVA followed by Dunnett's multiple comparison test. *n* refers to sample size. Significance was determined at $P<0.05$.

Acknowledgments

We acknowledge the invaluable help of several of our colleagues including Gerald Schatten for critical reading of the manuscript, discussion of the results, and financial support. Carrie Redinger and Jody Mich-Basso for hESC culture and RT PCR, Dave McFarland for help generating the teratomas, and John Ozolek for analysis of teratomas. Special thanks are due to Yuki Ohi and Miguel Ramalho-Santos (University of California, San Francisco) for invaluable assistance with experiments involving the WA09 cell line. We also thank Ana Sofia Rodrigues, Andre Tartar, Dan Constantinescu, and Charles Easley for critical reading of the manuscript. This work was supported by a grant from the National Institute of Child Health and Human Development, 1PO1HD047675 (to Gerald Schatten) and Fundacão para a Ciencia e Tecnologia (FCT) for scholarship support of S.V. J.-R.-S. was supported by a Fulbright Fellowship.

Appendix A. Supplementary data

Supplementary data associated with this article can be found, in the online version, at doi:10.1016/j.scr.2009.07.002.

References

Matsuda, T., Nakamura, T., Nakao, K., Arai, T., Katsuki, M., Heike, T., Yokota, T., 1999. STAT3 activation is sufficient to maintain an undifferentiated state of mouse embryonic stem cells. EMBO J. 18 (15), 4261–4269.

Niwa, H., Burdon, T., Chambers, I., Smith, A., 1998. Self-renewal of pluripotent embryonic stem cells is mediated via activation of STAT3. Genes Dev. 12 (13), 2048–2060.

Ying, Q.L., Nichols, J., Chambers, I., Smith, A., 2003. BMP induction of Id proteins suppresses differentiation and sustains embryonic stem cell self-renewal in collaboration with STAT3. Cell 115 (3), 281–292.

Daheron, L., Opitz, S.L., Zaehres, H., Lensch, M.W., Andrews, P.W., Itskovitz-Eldor, J., Daley, G.Q., 2004. LIF/STAT3 signaling fails to maintain self-renewal of human embryonic stem cells. Stem Cells 22 (5), 770–778.

Xu, R.H., Chen, X., Li, D.S., Li, R., Addicks, G.C., Glennon, C., Zwaka, T.P., Thomson, J.A., 2002. BMP4 initiates human embryonic stem cell differentiation to trophoblast. Nat. Biotechnol. 20 (12), 1261–1264.

Amit, M., Carpenter, M.K., Inokuma, M.S., Chiu, C.P., Harris, C.P., Waknitz, M.A., Itskovitz-Eldor, J., Thomson, J.A., 2000. Clonally derived human embryonic stem cell lines maintain pluripotency and proliferative potential for prolonged periods of culture. Dev. Biol. 227 (2), 271–278.

Rosler, E.S., Fisk, G.J., Ares, X., Irving, J., Miura, T., Rao, M.S., Carpenter, M.K., 2004. Long-term culture of human embryonic stem cells in feeder-free conditions. Dev. Dyn. 229 (2), 259–274.

Xu, C., Rosler, E., Jiang, J., Lebkowski, J.S., Gold, J.D., O'Sullivan, C., Delavan-Boorsma, K., Mok, M., Bronstein, A., Carpenter, M.K., 2005. Basic fibroblast growth factor supports undifferentiated human embryonic stem cell growth without conditioned medium. Stem Cells 23 (3), 315–323.

Wang, G., Zhang, H., Zhao, Y., Li, J., Cai, J., Wang, P., Meng, S., Feng, J., Miao, C., Ding, M., Li, D., Deng, H., 2005. Noggin and bFGF cooperate to maintain the pluripotency of human embryonic stem cells in the absence of feeder layers. Biochem. Biophys. Res. Commun. 330 (3), 934–942.

Xu, R.H., Peck, R.M., Li, D.S., Feng, X., Ludwig, T., Thomson, J.A., 2005. Basic FGF and suppression of BMP signaling sustain undifferentiated proliferation of human ES cells. Nat. Methods 2 (3), 185–190.

Vallier, L., Alexander, M., Pedersen, R.A., 2005. Activin/Nodal and FGF pathways cooperate to maintain pluripotency of human embryonic stem cells. J. Cell Sci. 118 (Pt. 19), 4495–4509.

Ezashi, T., Das, P., Roberts, R.M., 2005. Low O2 tensions and the prevention of differentiation of hES cells. Proc. Natl. Acad. Sci. USA 102 (13), 4783–4788.

Fischer, B., Bavister, B.D., 1993. Oxygen tension in the oviduct and uterus of rhesus monkeys, hamsters and rabbits. J. Reprod. Fertil 99 (2), 673–679.

St John, J.C., Ramalho-Santos, J., Gray, H.L., Petrosko, P., Rawe, V.Y., Navara, C.S., Simerly, C.R., Schatten, G.P., 2005. The expression of mitochondrial DNA transcription factors during early cardiomyocyte in vitro differentiation from human embryonic stem cells. Cloning Stem Cells 7 (3), 141–153.

Oh, S.K., Kim, H.S., Ahn, H.J., Seol, H.W., Kim, Y.Y., Park, Y.B., Yoon, C.J., Kim, D.W., Kim, S.H., Moon, S.Y., 2005. Derivation and characterization of new human embryonic stem cell lines: SNUhES1, SNUhES2, and SNUhES3. Stem Cells 23 (2), 211–219.

Cho, Y.M., Kwon, S., Pak, Y.K., Seol, H.W., Choi, Y.M., Park do, J., Park, K.S., Lee, H.K., 2006. Dynamic changes in mitochondrial biogenesis and antioxidant enzymes during the spontaneous differentiation of human embryonic stem cells. Biochem. Biophys. Res. Commun 348 (4), 1472–1478.

Chandel, N.S., McClintock, D.S., Feliciano, C.E., Wood, T.M., Melendez, J.A., Rodriguez, A.M., Schumacker, P.T., 2000. Reactive oxygen species generated at mitochondrial complex III stabilize hypoxia-inducible factor-1alpha during hypoxia: a mechanism of O2 sensing. J. Biol. Chem 275 (33), 25130–25138.

Guzy, R.D., Hoyos, B., Robin, E., Chen, H., Liu, L., Mansfield, K.D., Simon, M.C., Hammerling, U., Schumacker, P.T., 2005. Mitochondrial complex III is required for hypoxia-induced ROS production and cellular oxygen sensing. Cell Metab. 1 (6), 401–408.

Cauffman, G., Van de Velde, H., Liebaers, I., Van Steirteghem, A., 2005. Oct-4 mRNA levels and protein expression during human preimplantation development. Mol. Hum. Reprod. 11 (3), 173–181.

Eiselleova, L., Peterkova, I., Neradil, J., Slaninova, I., Hampl, A., Dvorak, P., 2008. Comparative study of mouse and human feeder cells for human embryonic stem cells. Int. J. Dev. Biol. 353–363.

Dvorak, P., Hampl, A., 2005. Basic fibroblast growth factor and its receptors in human embryonic stem cells. Folia Histochem. Cytobiol. 43 (4), 203–208.

Mohammadi, M., Froum, S., Hamby, J.M., Schroeder, M.C., Panek, R.L., Lu, G.H., Eliseenkova, A.V., Green, D., Schlessinger, J., Hubbard, S.R., 1998. Crystal structure of an angiogenesis inhibitor bound to the FGF receptor tyrosine kinase domain. EMBO J. 17 (20), 5896–5904.

Dvorak, P., Dvorakova, D., Koskova, S., Vodinska, M., Najvirtova, M., Krekac, D., Hampl, A., 2005. Expression and potential role of fibroblast growth factor 2 and its receptors in human embryonic stem cells. Stem Cells 23 (8), 1200–1211.

Adewumi, O., Aflatoonian, B., Ahrlund-Richter, L., Amit, M., Andrews, P.W., Beighton, G., Bello, P.A., Benvenisty, N., Berry, L.S., Bevan, S., Blum, B., Brooking, J., Chen, K.G., Choo, A.B., Churchill, G.A., Corbel, M., Damjanov, I., Draper, J.S., Dvorak, P., Emanuelsson, K., Fleck, R.A., Ford, A., Gertow, K., Gertsenstein, M., Gokhale, P.J., Hamilton, R.S., Hampl, A., Healy, L.E., Hovatta, O., Hyllner, J., Imreh, M.P., Itskovitz-Eldor, J., Jackson, J., Johnson, J.L., Jones, M., Kee, K., King, B.L., Knowles, B.B., Lako, M., Lebrin, F., Mallon, B.S., Manning, D., Mayshar, Y., McKay, R.D., Michalska, A.E., Mikkola, M., Mileikovsky, M., Minger, S.L., Moore, H.D., Mummery, C.L., Nagy, A., Nakatsuji, N., O'Brien, C.M., Oh, S.K., Olsson, C., Otonkoski, T., Park, K.Y., Passier, R., Patel, H., Patel, M., Pedersen, R., Pera, M.F., Piekarczyk, M.S., Pera, R.A., Reubinoff, B.E., Robins, A.J., Rossant, J., Rugg-Gunn, P., Schulz, T.C., Semb, H., Sherrer, E. S., Siemen, H., Stacey, G.N., Stojkovic, M., Suemori, H., Szatkiewicz, J., Turetsky, T., Tuuri, T., van den Brink, S., Vintersten, K., Vuoristo, S., Ward, D., Weaver, T.A., Young, L. A., Zhang, W., 2007. Characterization of human embryonic stem cell lines by the International Stem Cell Initiative. Nat. Biotechnol. 25 (7), 803–816.

Chambers, I., Colby, D., Robertson, M., Nichols, J., Lee, S., Tweedie, S., Smith, A., 2003. Functional expression cloning of Nanog, a pluripotency sustaining factor in embryonic stem cells. Cell 113 (5), 643–655.

Mitsui, K., Tokuzawa, Y., Itoh, H., Segawa, K., Murakami, M., Takahashi, K., Maruyama, M., Maeda, M., Yamanaka, S., 2003. The homeoprotein Nanog is required for maintenance of pluripotency in mouse epiblast and ES cells. Cell 113 (5), 631–642.

Nichols, J., Zevnik, B., Anastassiadis, K., Niwa, H., Klewe-Nebenius, D., Chambers, I., Scholer, H., Smith, A., 1998. Formation of pluripotent stem cells in the mammalian embryo depends on the POU transcription factor Oct4. Cell 95 (3), 379–391.

Baldassarre, G., Bianco, C., Tortora, G., Ruggiero, A., Moasser, M., Dmitrovsky, E., Bianco, A.R., Ciardiello, F., 1996. Transfection with a CRIPTO anti-sense plasmid suppresses endogenous CRIPTO expression and inhibits transformation in a human embryonal carcinoma cell line. Int. J. Cancer 66 (4), 538–543.

Vallier, L., Mendjan, S., Brown, S., Chng, Z., Teo, A., Smithers, L.E., Trotter, M.W., Cho, C.H., Martinez, A., Rugg-Gunn, P., Brons, G., Pedersen, R.A., 2009. Activin/Nodal signalling maintains pluripotency by controlling Nanog expression. Development 136 (8), 1339–1349.

Stern, C.D., 2005. Neural induction: old problem, new findings, yet more questions. Development 132 (9), 2007–2021.

Westfall, S.D., Sachdev, S., Das, P., Hearne, L.B., Hannink, M., Roberts, R.M., Ezashi, T., 2008. Identification of oxygen-sensitive transcriptional programs in human embryonic stem cells. Stem Cells Dev. 17 (5), 869–881.

Darr, H., Mayshar, Y., Benvenisty, N., 2006. Overexpression of NANOG in human ES cells enables feeder-free growth while inducing primitive ectoderm features. Development 133 (6), 1193–1201.

Xu, R.H., Sampsell-Barron, T.L., Gu, F., Root, S., Peck, R.M., Pan, G., Yu, J., Antosiewicz-Bourget, J., Tian, S., Stewart, R., Thomson, J.A., 2008. NANOG is a direct target of TGFbeta/activin-mediated SMAD signaling in human ESCs. Cell Stem Cell 3 (2), 196–206.

Rodriguez, R.T., Velkey, J.M., Lutzko, C., Seerke, R., Kohn, D.B., O'Shea, K.S., Firpo, M.T., 2007. Manipulation of OCT4 levels in human embryonic stem cells results in induction of differential cell types. Exp. Biol. Med. (Maywood) 232 (10), 1368–1380.

Niwa, H., Miyazaki, J., Smith, A.G., 2000. Quantitative expression of Oct-3/4 defines differentiation, dedifferentiation or self-renewal of ES cells. Nat. Genet. 24 (4), 372–376.

Hay, D.C., Sutherland, L., Clark, J., Burdon, T., 2004. Oct-4 knockdown induces similar patterns of endoderm and trophoblast differentiation markers in human and mouse embryonic stem cells. Stem Cells 22 (2), 225–235.

Velkey, J.M., O'Shea, K.S., Oct4, R.N.A., 2003. interference induces trophectoderm differentiation in mouse embryonic stem cells. Genesis 37 (1), 18–24.

Matin, M.M., Walsh, J.R., Gokhale, P.J., Draper, J.S., Bahrami, A.R., Morton, I., Moore, H.D., Andrews, P.W., 2004. Specific knockdown of Oct4 and beta2-microglobulin expression by RNA interference in human embryonic stem cells and embryonic carcinoma cells. Stem Cells 22 (5), 659–668.

Pan, G., Li, J., Zhou, Y., Zheng, H., Pei, D., 2006. A negative feedback loop of transcription factors that controls stem cell pluripotency and self-renewal. FASEB J 20 (10), 1730–1732.

Ramalho-Santos, J., Varum, S., Amaral, S., Mota, P.C., Sousa, A.P., Amaral, A., 2009. Mitochondrial functionality in reproduction: from gonads and gametes to embryos and embryonic stem cells. Hum. Reprod. 15 (5), 553–572.

Stern, S., Biggers, J.D., Anderson, E., 1971. Mitochondria and early development of the mouse. J. Exp. Zool. 176 (2), 179–191.

Houghton, F.D., 2006. Energy metabolism of the inner cell mass and trophectoderm of the mouse blastocyst. Differentiation 74 (1), 11–18.

Finkel, T., 2003. Oxidant signals and oxidative stress. Curr. Opin. Cell Biol. 15 (2), 247–254.

Carriere, A., Carmona, M.C., Fernandez, Y., Rigoulet, M., Wenger, R. H., Penicaud, L., Casteilla, L., 2004. Mitochondrial reactive oxygen species control the transcription factor CHOP-10/GADD153 and adipocyte differentiation: a mechanism for hypoxia-dependent effect. J. Biol. Chem. 279 (39), 40462–40469.

Thannickal, V.J., Fanburg, B.L., 2000. Reactive oxygen species in cell signaling. Am. J. Physiol. Lung Cell Mol. Physiol. 279 (6), L1005–L1028.

Chung, S., Dzeja, P.P., Faustino, R.S., Perez-Terzic, C., Behfar, A., Terzic, A., 2007. Mitochondrial oxidative metabolism is required for the cardiac differentiation of stem cells. Nat. Clin. Pract. Cardiovasc. Med. 4 (Suppl. 1), S60–S67.

Spitkovsky, D., Sasse, P., Kolossov, E., Bottinger, C., Fleischmann, B.K., Hescheler, J., Wiesner, R.J., 2004. Activity of complex III of the mitochondrial electron transport chain is essential for

early heart muscle cell differentiation. FASEB J. 18 (11), 1300–1302.
Xu, C., Inokuma, M.S., Denham, J., Golds, K., Kundu, P., Gold, J.D., Carpenter, M.K., 2001. Feeder-free growth of undifferentiated human embryonic stem cells. Nat. Biotechnol. 19 (10), 971–974.
Ying, Q.L., Wray, J., Nichols, J., Batlle-Morera, L., Doble, B., Woodgett, J., Cohen, P., Smith, A., 2008. The ground state of embryonic stem cell self-renewal. Nature 453 (7194), 519–523.
Navara, C.S., Redinger, C., Mich-Basso, J., Oliver, S., Ben-Yehudah, A., Castro, C., Simerly, C., 2007. Derivation and characterization of nonhuman primate embryonic stem cells. Curr. Protoc. Stem Cell Biol. Chap. 1, Unit 1A 1.
Amaral, S., Moreno, A.J., Santos, M.S., Seica, R., Ramalho-Santos, J., 2006. Effects of hyperglycemia on sperm and testicular cells of Goto-Kakizaki and streptozotocin-treated rat models for diabetes. Theriogenology 66 (9), 2056–2067.